The Astrophysical Journal, 672:59–71, 2008 January 1

ON THE NATURE OF VELOCITY FIELDS IN HIGH-z GALAXIES

Jason X. Prochaska,[1] Hsiao-Wen Chen,[2] Arthur M. Wolfe,[3]
Miroslava Dessauges-Zavadsky,[4] and Joshua S. Bloom[5]
Received 2007 March 27; accepted 2007 August 31

ABSTRACT

We analyze the gas kinematics of damped Lyα systems (DLAs) hosting high-z gamma-ray bursts (GRBs) and those toward quasars (QSO-DLAs), focusing on three statistics: (1) Δv_{90}, the velocity interval encompassing 90% of the integrated optical depth, and (2) W_{1526} and (3) W_{1548}, the rest equivalent widths of the Si II 1526 and C IV 1548 transitions, respectively. The Δv_{90} distributions of the GRB-DLAs and QSO-DLAs are similar; each has median $\Delta v_{90} \approx 80$ km s^{-1} and a significant tail, extending to several hundred km s^{-1}. This suggests comparable galaxy masses for the parent populations of GRB-DLAs and QSO-DLAs, and we infer that the average dark matter halo mass of GRB galaxies is $\lesssim 10^{12}\ M_{\odot}$. The unique configuration of GRB-DLA sight lines and the presence (and absence) of fine-structure absorption together give special insight into the nature of high-z protogalactic velocity fields. The data support a scenario in which the Δv_{90} statistic reflects dynamics in the interstellar medium (ISM) and W_{1526} traces motions outside the ISM (e.g., halo gas and galactic-scale winds). The W_{1526} statistic and gas metallicity [M/H] are tightly correlated, especially for the QSO-DLAs: $[\mathrm{M/H}] = a + b \log (W_{1526}/1\ \text{Å})$ with $a = -0.92 \pm 0.05$ and $b = 1.41 \pm 0.10$. We argue that the W_{1526} statistic primarily tracks dynamical motions in the halos of high-z galaxies and interpret this correlation as a mass-metallicity relation with very similar slope to the trend observed in local, low-metallicity galaxies. Finally, the GRB-DLAs exhibit systematically larger W_{1526} values (>0.5 Å) than the QSO-DLAs ($\langle W_{1526} \rangle \approx 0.5$ Å), which may suggest that galactic-scale outflows contribute to the largest observed velocity fields.

Subject heading: quasars: absorption lines

Online material: color figures

1. INTRODUCTION

Absorption-line spectra of quasars have revealed thousands of high-redshift galaxies to date (e.g., Wolfe et al. 1986; Steidel & Sargent 1992; Prochaska et al. 2005; Prochter et al. 2006). If traced by the Lyα transition, these galaxies are termed the damped Lyα systems (DLAs), absorbers with H I column density $N_{\mathrm{H\,I}} \geq 2 \times 10^{20}$ cm^{-2}. Although a direct association between star-forming galaxies and DLAs is difficult to establish, because the background quasar blinds our view (Møller et al. 2002), the large $N_{\mathrm{H\,I}}$ values of DLAs indicate very large dark matter overdensities (i.e., a virialized system). Furthermore, all of the DLAs show substantial enrichment from heavy metals (Pettini et al. 1994; Prochaska et al. 2003), and roughly half show indications of ongoing star formation through the presence of C II* absorption (Wolfe et al. 2003). Finally, stars form from neutral gas, and the DLAs dominate the atomic hydrogen reservoir at all redshifts (Wolfe et al. 1995; Prochaska et al. 2005; Rao et al. 2006).

High-resolution spectroscopy of DLAs yields precise measurements of the column densities of resonance line transitions in the ISM of high-z galaxies (Wolfe et al. 2005). Aside from gas-phase abundances, however, it is difficult to derive physical quantities from these observations (e.g., temperature and density). The only other physical characteristic easily studied is the gas kinematics. High-resolution spectra resolve the line profiles of these transitions into "clouds" that trace the velocity fields in young, high-z galaxies (Prochaska & Wolfe 1997, 1998). Although it is difficult to reveal the nature of these velocity fields (e.g., rotation, outflows, and turbulence) with individual one-dimensional sight lines, the distributions of kinematic characteristics provide powerful tests for scenarios of galaxy formation (e.g., Jedamzik & Prochaska 1998; Haehnelt et al. 1998).

Prochaska & Wolfe (1997) performed a survey of the kinematic characteristics of neutral gas in DLAs and compared their observations against a variety of simple scenarios. These included rotating disks, clouds with random (virialized) motions, and galactic infall. Observed asymmetries in the observed line profiles favor rotational dynamics, yet the observed distribution of velocity widths (Δv) has a median too large to be accommodated within standard cold dark matter cosmology. As such, Prochaska & Wolfe (1997) presented these observations as a direct challenge to the basic picture of galaxy formation in a hierarchical universe (e.g., Kauffmann 1996; Mo et al. 1998). In response, theorists introduced additional velocity fields to explain the observations (Haehnelt et al. 1998; McDonald & Miralda-Escudé 1999; Nulsen et al. 1998; Maller et al. 2001). Of particular interest was a model of merging protogalactic clumps in which the observed kinematics include contributions from rotation, infall, and random motions (Haehnelt et al. 1998). While the initial work established this model as a potential solution, recent evaluations using modern numerical simulations and more accurate treatments of radiative transfer have not confirmed its viability (Prochaska & Wolfe 2001; Razoumov et al. 2006).

Motivated by these results, we have investigated the dynamics of gas probed by the sight lines to the afterglows of gamma-ray bursts (GRBs). Similar to quasars, the afterglows of GRBs provide bright, albeit transient, point-source beacons to the outer

[1] Department of Astronomy and Astrophysics, UCO/Lick Observatory; University of California, 1156 High Street, Santa Cruz, CA 95064; xavier@ucolick.org.
[2] Department of Astronomy, University of Chicago, 5640 South Ellis Avenue, Chicago, IL 60637; hchen@oddjob.uchicago.edu.
[3] Department of Physics, and Center for Astrophysics and Space Sciences, University of California, San Diego, C–0424, La Jolla, CA 92093-0424.
[4] Observatoire de Genève, 51 Ch. des Maillettes, 1290 Sauverny, Switzerland.
[5] Department of Astronomy, 601 Campbell Hall, University of California, Berkeley, CA 94720-3411.

universe. With follow-up spectroscopy, one can acquire data at signal-to-noise ratio (S/N) and spectral resolution comparable to quasars (Vreeswijk et al. 2004; Fiore et al. 2005; Chen et al. 2005; Prochaska et al. 2007b). In turn, one can study the velocity fields of the gas close to the observed beacon. The sight line presumably intersects gas in the star-forming region encompassing the GRB, the neutral ISM surrounding it, and gas external to the neutral ISM.

In this paper, we examine the kinematics of a modest sample of damped Lyα systems associated with the ISM surrounding gamma-ray bursts (GRB-DLAs). A principal goal is to characterize the velocity fields of gas observed along these unique sight lines. The data trace velocity fields generated by galactic rotation, gravitational accretion, and any galactic or stellar feedback processes. We find that these observations reveal new insight for interpretations of the kinematics of gas observed in quasar absorption-line studies. Furthermore, we present a comparison of the GRB-DLA results with those from DLAs toward QSOs (QSO-DLAs). Comparisons between GRB-DLAs and QSO-DLAs assess the relative galaxy masses and the nature of velocity fields in young, star-forming galaxies.

This paper is organized as follows. Section 2 presents the observational samples and describes the experiment. In § 3, we define statistics for assessing the gas kinematics. Section 4 presents the principal results of our analysis, and we discuss and interpret these results in § 5.

2. OBSERVATIONAL DATA

We have defined a sample of GRB-DLAs for kinematic analysis based on two primary criteria: (1) the presence of a damped Lyα system ($N_{\rm H\,I} \geq 2 \times 10^{20}$ cm^{-2}) or a low-ion column density that requires that $N_{\rm H\,I}$ exceed 2×10^{20} cm^{-2} assuming solar metallicity and (2) spectra with sufficient signal-to-noise ratio and resolution to study the gas kinematics. The latter criterion is not especially strict, because we examine the gas kinematics from equivalent width measurements that do not require high spectral resolution. The sample is also limited to GRB-DLAs for which we could access the data or for which precise equivalent width measurements are reported in the literature. Figure 1 shows an example set of line profiles for the GRB-DLA associated with GRB 050820 (Prochaska et al. 2007b). These data were acquired with the HIRES spectrometer on the Keck telescope and have high spectral resolution ($R \approx 40{,}000$). The weaker transitions, such as Zn II 2026, indicate that most (90%) of the gas is localized to one or two "clouds" within a velocity interval of $\approx$50 km s^{-1}. In contrast, the stronger transitions are typically saturated and show absorption spanning nearly 400 km s^{-1}. In § 3 we introduce two kinematic statistics to characterize these properties. Table 1 lists the GRB-DLAs composing our sample, describes the spectral observations, and lists the $N_{\rm H\,I}$ values and metallicities as described in Prochaska et al. (2007a).

Our analysis frequently draws comparisons between GRB-DLA measurements and QSO-DLA values. For the latter, we consider two samples of QSO-DLAs, one a subset of the other. The complete sample is drawn from echelle and echellette observations of quasars acquired with the HIRES (Vogt et al. 1994) and ESI (Sheinis et al. 2000) spectrometers at the Keck Observatory and the UVES (Dekker et al. 2000) spectrometer at the VLT Observatory. The data are summarized in these papers: Herbert-Fort et al. (2006), Ledoux et al. (2006), Dessauges-Zavadsky et al. (2006), and Prochaska et al. (2007a). We restrict the samples to $z_{\rm DLA} > 1.6$ and DLAs that are more than 3000 km s^{-1} from their background quasar. The full data set is a heterogeneous sample of QSO-DLAs including systems selected on the basis of strong metal lines (Herbert-Fort et al. 2006) or targeted for H_2 absorption (Ledoux et al. 2003). As such, Prochaska et al. (2007b) have noted that the H I distribution $f(N_{\rm H\,I})$ of this full sample does not follow the statistical distribution[6] derived from a random survey of background quasars (e.g., Prochaska et al. 2005). Therefore, we define a pseudostatistical sample of QSO-DLAs by restricting the list to the QSO-DLAs compiled by Prochaska et al. (2003). Although the DLAs in this subset also do not follow the $f(N_{\rm H\,I})$ distribution of a random sample, they were selected only on the basis of a large H I column density, i.e., independent of any kinematic characteristic or chemical abundance.

We have analyzed the kinematic properties from our own HIRES and ESI observations and supplemented these measurements with the results presented in Ledoux et al. (2006) from UVES data acquired with the VLT. For equivalent width measurements, however, we have derived values only from our HIRES and ESI observations (Prochaska et al. 2007a; Herbert-Fort et al. 2006). These values have typical statistical uncertainties of less than 0.02 Å.

In a previous paper (Prochaska et al. 2007a), we discussed why the parent populations of galaxies hosting QSO-DLAs and GRB-DLAs may be different (e.g., gas cross section selected vs. current star formation rate [SFR] selected) and how the sight-line configurations are fundamentally distinct. The GRB-DLAs do exhibit larger $N_{\rm H\,I}$, metallicity, α/Fe, and depletion levels than QSO-DLAs (Prochaska et al. 2007a), but we argued that the differences do not require distinct parent populations of galaxies. Instead, the GRB-DLA observations are readily explained by sight lines with smaller average impact parameter through the same population of high-z galaxies. This conclusion is expected for a sample selected by gas cross section (QSO-DLA) versus ones restricted to originate in star-forming regions (GRB-DLA). The cartoon in Figure 2 illustrates these ideas. While QSO-DLAs preferentially penetrate the outer regions of the ISM, the GRB-DLA sight lines originate within their host galaxies, presumably within an H II region generated by its progenitor and other O and B stars. This has two key implications for the gas kinematics: (1) the GRB-DLA observations will probe only a fraction of the velocity field along the full sight line, and (2) each GRB-DLA sight line is biased to intersect its own star-forming region. We expect these regions to have very small cross section to QSO-DLA sight lines (Zwaan & Prochaska 2006) and to be rarely probed by such samples. In this respect, GRB-DLAs may open a new window into the velocity fields of high-z galaxies (cf. Pettini et al. 2001).

3. KINEMATIC DIAGNOSTICS

With high-resolution observations, one resolves the absorption-line profiles of unsaturated transitions into individual components, frequently termed "clouds." The clouds in QSO-DLAs have typical Doppler widths of $b = \sqrt{2}\sigma \approx 5$–$10$ km s^{-1} (e.g., Dessauges-Zavadsky et al. 2006). The dispersion is expected to result from macroscopic motions (e.g., turbulence) and not only thermal broadening; for $b \approx 10$ km s^{-1}, the latter would imply temperatures that would collisionally ionize the gas. The GRB-DLAs show clouds with similar characteristics that comprise the observed line profiles (Fig. 1; Fiore et al. 2005; Chen et al. 2005; Prochaska et al. 2007b).

One can characterize the velocity field along the sight line by tracing the motions of these clouds. Presently, we do not have

[6] The QSO-DLAs observed at high spectral resolution have systematically fewer systems with $N_{\rm H\,I} \approx 2 \times 10^{20}$ cm^{-2}, presumably because the observers wished to avoid including absorbers right at the threshold.

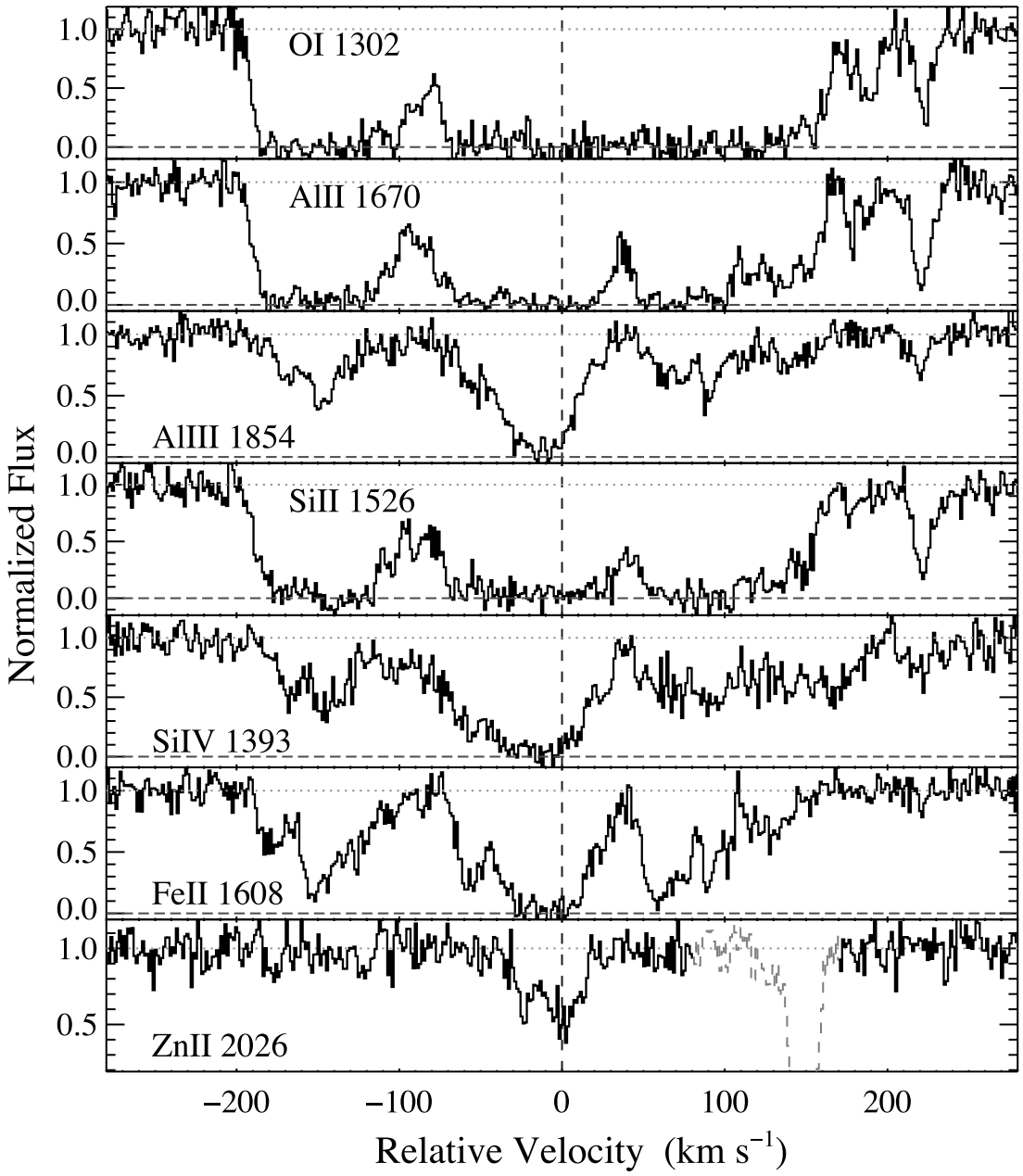

FIG. 1.—Resonance line profiles for the GRB-DLA associated with GRB 050820 (Prochaska et al. 2007b). The velocity $v = 0$ corresponds to $z = 2.61469$. Note that the optical depth in low-ion gas is dominated by a few clouds with velocity interval $\Delta v_{90} \approx 50$ km s^{-1} (Zn II 2026). At the same time, there is absorption traced by strong low-ion transitions (e.g., Si II 1526) to velocities of $\approx \pm 200$ km s^{-1}. [*See the electronic edition of the Journal for a color version of this figure.*]

measurements of the systemic redshifts for our sample of GRB host galaxies (e.g., via nebular lines). Therefore, we primarily discuss relative velocities. Standard practice is to define a velocity width Δv_{90} as the interval that encompasses 90% of the integrated optical depth of the gas. This definition was introduced in part to limit a single, weak cloud or statistical fluctuations from dominating the statistic (Prochaska & Wolfe 1997). Following the approach for QSO-DLAs (Prochaska & Wolfe 1997, 1998, 2001; Ledoux et al. 2006), we measure the Δv_{90} statistic from a single, unsaturated low-ion transition[7] that, ideally, has relatively high S/N. For the QSO-DLAs we demand S/N > 15 pixel^{-1}, but have relaxed this requirement for the GRB-DLAs because of the generally poorer data quality. To resolve the optical depth profile, however, it is necessary to restrict the sample to echelle or echellette observations. As an example of the procedure, consider the line profiles in Figure 1, where we measure $\Delta v_{90} = 55$ km s^{-1} using the Zn II λ2026 transition.

Table 2 summarizes the measurements for the full GRB-DLA sample. These include three Δv_{90} measurements obtained from Keck ESI spectroscopy with FWHM ≈ 45 km s^{-1}. We have tested the effects of using these lower resolution observations by smoothing our Keck HIRES observations to the ESI resolution, adding noise, and then comparing the Δv_{90} values. We find that Δv_{90} is biased high by a little less than half the FWHM (20 km s^{-1}), because the edges of the velocity interval are artificially broadened. Therefore, we have reduced the Δv_{90} values from the Keck ESI observations by 20 km s^{-1} to account for this systematic effect. We estimate the uncertainty in the Δv_{90} values to be 20 km s^{-1} for the Keck ESI data and $\approx$10 km s^{-1} for all other measurements.

[7] Note that Δv_{90} is insensitive to the specific transition analyzed, provided the line is unsaturated and is associated with a low ion (Prochaska & Wolfe 1997).

TABLE 1
GRB-DLA Sample

GRB	R.A.	Decl.	z_{GRB}	$\log N_{H\,I}$	f_{mtl}[a]	[M/H][b]	σ([M/H])	Instrument	R	Reference
GRB 990123	15 25 30.34	+44 45 59.1	1.600	...	...	...	...	Keck LRIS	1000	1
GRB 000926	17 04 09.00	+51 47 10.0	2.038	$21.30^{+0.25}_{-0.25}$	2	−0.17	0.29	Keck ESI	5000	2
GRB 010222	14 52 12.55	+43 01 06.2	1.477	...	...	...	...	Keck ESI	5000	3
GRB 011211	11 15 17.98	−21 56 56.2	2.142	$20.40^{+0.20}_{-0.20}$	11	−1.36	...	VLT/FORS2	1000	1,4
GRB 020813	19 46 41.87	−19 36 04.8	1.255	...	...	...	...	Keck LRIS, VLT UVES	1000; 30,000	5,6
GRB 030226	11 33 04.93	+25 53 55.3	1.987	$20.50^{+0.30}_{-0.30}$	11	−1.31	...	Keck ESI	5000	7
GRB 030323	11 06 09.40	−21 46 13.2	3.372	$21.90^{+0.07}_{-0.07}$	12	−0.87	...	VLT FORS2	1000	8
GRB 050401	16 31 28.82	+02 11 14.8	2.899	$22.60^{+0.30}_{-0.30}$	12	−1.57	...	VLT FORS2	1000	9
GRB 050505	09 27 03.20	+30 16 21.5	4.275	$22.05^{+0.10}_{-0.10}$	11	−1.25	...	Keck/LRIS	1000	10
GRB 050730	14 08 17.14	−03 46 17.8	3.969	$22.15^{+0.10}_{-0.10}$	4	−2.26	0.14	Magellan MIKE	30,000	11
GRB 050820	22 29 38.11	+19 33 37.1	2.615	$21.00^{+0.10}_{-0.10}$	4	−0.63	0.11	Keck HIRES	30,000	12
GRB 050904	00 54 50.79	+14 05 09.4	6.296	$21.30^{+0.20}_{-0.20}$	11	−1.10	...	Subaru FOCAS	1000	13
GRB 050922C	19 55 54.48	−08 45 27.5	2.199	$21.60^{+0.10}_{-0.10}$	4	−2.03	0.14	VLT UVES	30,000	14
GRB 051111	00 08 17.14	−00 46 17.8	1.549	...	...	...	...	Keck HIRES	30,000	15,12
GRB 060206	13 31 43.42	+35 03 03.6	4.048	$20.85^{+0.10}_{-0.10}$	4	−0.85	0.18	WHT ISIS	4000	16
GRB 060418	15 45 42.40	−03 38 22.80	1.490	...	...	...	...	Magellan MIKE	30,000	12

Note.—Units of right ascension are hours, minutes, and seconds, and units of declination are degrees, arcminutes, and arcseconds.
[a] Flag describing the metallicity measurement [M/H]: (2) Zn measurement; (4) S measurement; (11) lower limit from [α/H]; (12) lower limit from Zn.
[b] Metallicity value reported by Prochaska et al. (2007a). The lower limits correspond to observed equivalent widths assuming the weak limit of the curve of growth.
References.—(1) Savaglio et al. 2003; (2) Castro et al. 2003; (3) Mirabal et al. 2002; (4) Vreeswijk et al. 2006; (5) Barth et al. 2003; (6) Fiore et al. 2005; (7) Shin et al. 2006; (8) Vreeswijk et al. 2004; (9) Watson et al. 2006; (10) Berger et al. 2006; (11) Chen et al. 2005; (12) Prochaska et al. 2007b; (13) Kawai et al. 2006; (14) S. Piranomonte et al. 2007, in preparation; (15) Prochaska et al. 2006; (16) Fynbo et al. 2006.

We also introduce a complimentary diagnostic of gas kinematics, the rest equivalent width $W = W_{obs}/(1+z)$. This quantity has kinematic significance for optically thick (i.e., saturated) transitions. In these cases, the equivalent width is most sensitive to the differential motions of individual clouds as opposed to their column densities. In contrast to Δv_{90}, the W value represents the velocity field of greater than 90% of the gas and can be dominated by clouds with relatively low column density (e.g., Boucle et al. 2007). We emphasize that the W value should only be sensitive to the metallicity and/or $N_{H\,I}$ value of the sight line at very low values, i.e., when the transition is not saturated. Below, we demonstrate that Δv_{90} and W are correlated, but with large scatter.

We have measured rest equivalent widths from the Si II λ1526 transition (W_{1526}) for low-ion gas and the C IV 1548 transition for high-ion gas. The Si II λ1526 transition saturates at $N(Si^+) \approx 10^{14}$ cm^{-2},which is 10 times lower than the Si^+ column density for any GRB-DLA sight line and 2 times lower than nearly every QSO-DLA. Therefore, this measure should be relatively insensitive to the gas metallicity or the $N_{H\,I}$ value. This point is emphasized in Figure 3, where we show the curve of growth for the Si II 1526 transition and the observed total Si^+ column density and equivalent widths for the QSO-DLAs and GRB-DLAs. It is evident that the equivalent width has significant contributions from multiple, lower column density clouds. Because C IV is a doublet, the C IV 1548 transition will blend with C IV 1550 when $W_{1548} \gtrsim 2$ Å. In these few cases, we adopt a lower limit for W_{1548}. The W_{1526} and W_{1548} values of the GRB-DLAs are summarized in Table 2. We also list the metallicity [M/H] measurement (or

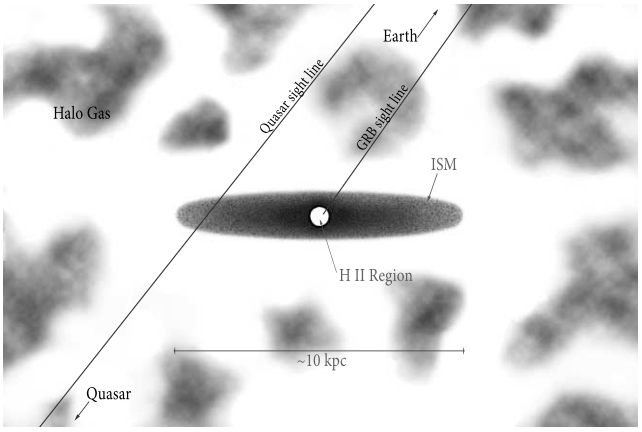

Fig. 2.—Cartoon illustrating the likely differences between QSO-DLA and GRB-DLA sight lines. The former have randomly intersected a foreground galaxy. These QSO-DLA sight lines correspond to a cross section–selected sample and should preferentially intersect the outer regions of the ISM in high-z galaxies. In contrast, the GRB-DLA sight lines are constrained to originate from within the ISM of their host galaxies, presumably the H II region produced by massive stars in a star-forming region. These GRB-DLA sight lines are expected (and observed) to originate within the inner few kpc of the ISM.

TABLE 2
GRB-DLA Kinematic Characteristics Summary

GRB	λ_{low} (Å)	Δv_{90} (km s^{-1})	W_{1526} (Å)	W_{1548} (Å)
GRB 000926	2026.136	260[a]	2.40 ± 0.14	>2.20
GRB 010222	2056.254	80[a]	1.51 ± 0.13	>2.55
GRB 011211	...	...	1.35 ± 0.19	0.70 ± 0.13
GRB 020813	2260.780	210	1.71 ± 0.10	1.53 ± 0.05
GRB 030226	2374.461	295[a,b]	0.97 ± 0.02	0.32 ± 0.02
GRB 030323	...	...	0.75 ± 0.03	1.50 ± 0.03
GRB 050401	...	...	2.31 ± 0.26	1.28 ± 0.26
GRB 050505	...	...	1.81 ± 0.10	>5.92
GRB 050730	1741.553	25	0.37 ± 0.01	0.81 ± 0.01
GRB 050820	2026.136	55	1.65 ± 0.01	1.51 ± 0.01
GRB 050922C	1608.451	89	0.52 ± 0.01	0.75 ± 0.01
GRB 051111	2249.877	31	0.79 ± 0.20	1.35 ± 0.20
GRB 060418	2576.877	57	0.66 ± 0.02	0.80 ± 0.02

Note.—All EW values reported are rest-frame equivalent widths.
[a] Corrected downward by 20 km s^{-1} because the observations were performed with Keck ESI. See the text for an explanation.
[b] Estimated from Fig. 2 of Shin et al. (2006). Because the line profiles are partially saturated, this value may be considered an upper limit.

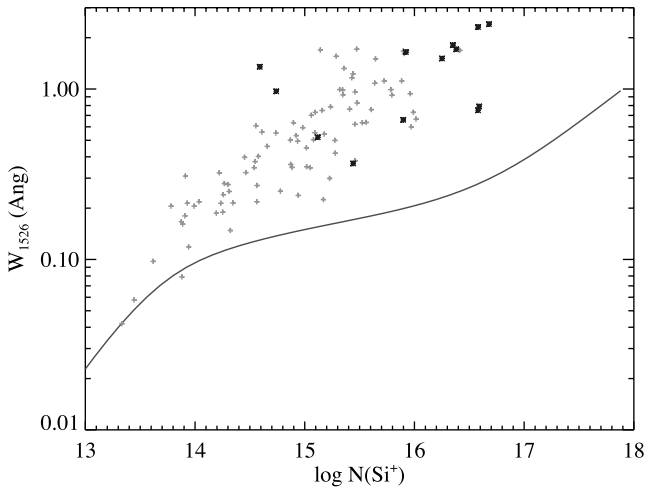

FIG. 3.—Curve of growth for the Si II 1526 transition, assuming a Doppler parameter $b = 7$ km s^{-1}. Overplotted on the figure are the observed total Si$^+$ column densities and equivalent widths from the QSO-DLAs (*plus signs*) and GRB-DLAs (*stars*). Aside from the few QSO-DLAs with very low W_{1526}, the equivalent widths are dominated by the contribution from multiple clouds with a broad range of column densities. [*See the electronic edition of the Journal for a color version of this figure.*]

lower limit) for each GRB-DLA (see Prochaska et al. 2007a for details).

4. RESULTS

In this section, we present the observational results. Section 5 discusses the implications.

4.1. Δv_{90} *and* W_{1526} *Distributions*

Figure 4*a* presents the velocity width (Δv_{90}) distributions for the GRB-DLAs and for the statistical subset of QSO-DLAs. The two distributions are similar; the majority of galaxies have $\Delta v_{90} < 100$ km s^{-1}, and each sample shows a tail out to several hundred km s^{-1}. A two-sided Kolmogorov-Smirnov (K-S) test rules out the null hypothesis that the two distributions are drawn from the same parent population at only 68% CL (confidence level). In the current GRB-DLA sample, there is a higher fraction of systems with $\Delta v_{90} > 200$ km s^{-1} than the QSO-DLA distribution. The difference is not statistically significant at present, but future observations may reveal a systematic difference in this respect.

Because the GRBs are embedded within the interstellar medium (Fig. 2), the velocity widths are likely an underestimate of the value that one would derive by extending the sight line through the other side of the galaxy. If the kinematics are dominated by random motions or rotational dynamics, then the median increase in Δv_{90} should be less than a factor of 2. To be conservative, we have recomputed the K-S statistic after doubling each Δv_{90} value of the GRB-DLAs. We find results that are still consistent with the null hypothesis, $P_{\text{K-S}} = 0.05$. In this regard, the sample of GRB-DLA sight lines have velocity fields typical of those observed for QSO-DLAs. Under the assumption that Δv_{90} is dominated by the gravitational potential (e.g., Haehnelt et al. 1998), these results suggest that the parent populations of GRB-DLAs and QSO-DLAs have similar dynamical masses.

From even the first afterglow spectrum (Metzger et al. 1997), it was evident that the gas surrounding GRBs exhibits large equivalent widths from low-ion transitions such as Si II λ1526 and Mg II λ2796 (Savaglio et al. 2003). As noted in § 3, these large equivalent widths do not require large $N_{\text{H I}}$ or metallicity; the values are

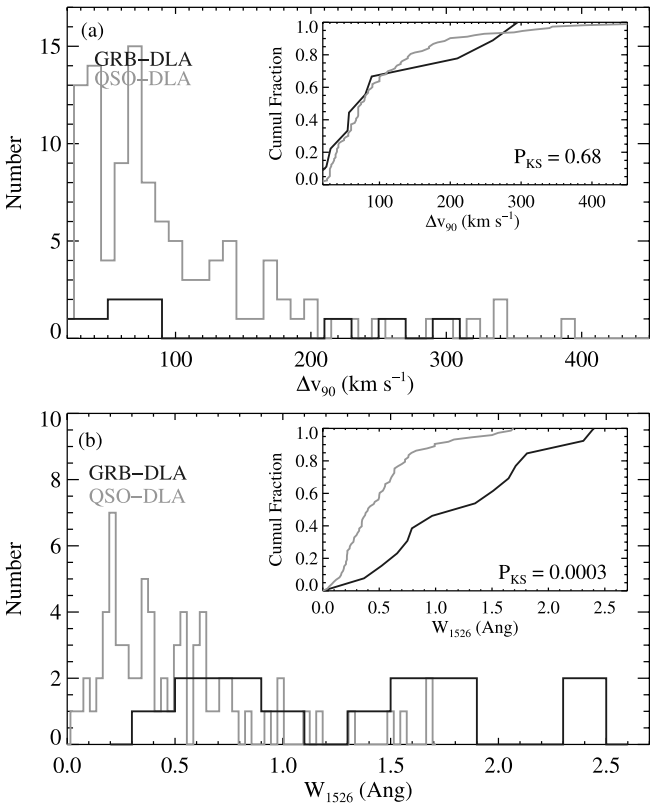

FIG. 4.—Histograms of low-ion kinematic statistics for the GRB-DLAs (*black*) compared against a statistical sample of QSO-DLAs (*gray*). (*a*) Results for the Δv_{90} statistic, the velocity interval containing 90% of the optical depth of the low-ion gas. The two samples have similar distributions, with median $\Delta v_{90} \approx 80$ km s^{-1} and a significant tail, extending to several hundred km s^{-1}. (*b*) Equivalent widths of the Si II 1526 transition. In contrast to the Δv_{90} statistic, the GRB-DLAs exhibit systematically larger W_{1526} values than the QSO-DLAs. In each panel, the inset shows the cumulative distributions of the systems, normalized to unity, and the $P_{\text{K-S}}$ value gives the probability that the two distributions are drawn from the same parent population. [*See the electronic edition of the Journal for a color version of this figure.*]

often dominated by the velocity fields of low column density clouds, which do not contribute to the Δv_{90} statistic. Figure 4*b* presents a histogram of W_{1526} values for the GRB-DLAs compared to the values of the statistical QSO-DLA subset. The mean and median of the GRB-DLA distributions are significantly larger than the QSO-DLAs, and a K-S test rules out the null hypothesis at 99.9% CL. Whereas the Δv_{90} values are in rather good agreement between the two samples, the W_{1526} values of the GRB-DLAs are systematically larger. This is an unexpected and puzzling result, which requires unique velocity fields from low column density gas along GRB sight lines.

We argue below that the Δv_{90} statistic in GRB-DLAs is dominated by the neutral ISM of the GRB host galaxy. It is our expectation that this also holds true for QSO-DLAs. We also argue that the W_{1526} values result from motions independent of the neutral ISM. If other environments contribute to W_{1526}, then one predicts Δv_{90} to be only loosely correlated with W_{1526}. Figure 5, which plots Δv_{90},W_{1526} pairs for the GRB-DLAs and QSO-DLAs, indicates that this is the case. The dashed line traces the predicted W_{1526} value for a fully saturated (i.e., boxcar) line profile that has velocity width Δv_{90}. Although the QSO-DLAs roughly follow this line, the GRB-DLAs tend to lie significantly above it. Regarding the QSO-DLAs, we interpret the results in Figure 5 as evidence that many sight lines penetrate gas with velocity fields that are distinct from the majority of gas. In the GRB-DLAs, nearly

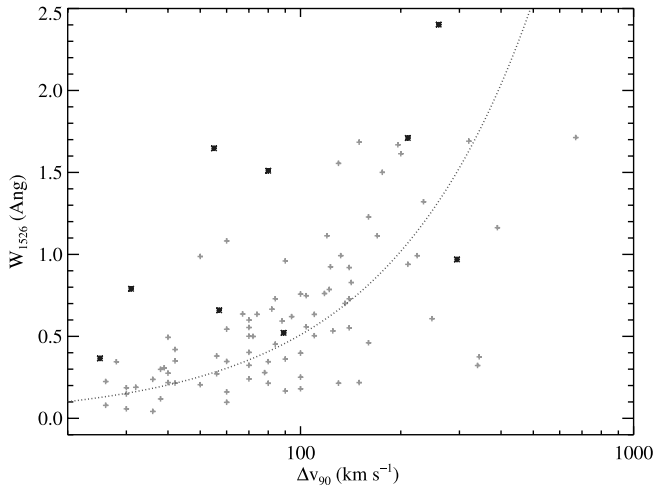

FIG. 5.—Plot of Δv_{90}, W_{1526} pairs for the QSO-DLAs (*gray*) and GRB-DLAs (*black*) samples. The dashed line indicates the W_{1526} value for a boxcar line profile with velocity width Δv_{90}, i.e., $W_{1526} = \Delta v_{90} 1526.7066/c$. The sight lines that lie significantly above this curve must have contributions to W_{1526} from gas at large velocity and with less than 10% of the optical depth. The typical error in the QSO-DLA W_{1526} values is less than a few times 10 mÅ. [*See the electronic edition of the Journal for a color version of this figure.*]

every sight line shows a substantial contribution to W_{1526} from gas that does not dominate the integrated optical depth. In § 5, we discuss the origin and nature of these velocity fields in greater detail.

4.2. *Kinematic Correlations with Other Properties of the ISM*

We have considered the trends between kinematic characteristics and other physical properties of the ISM. We first examined whether the GRB-DLAs follow the observed trends for QSO-DLAs between gas kinematics and metallicity (Wolfe & Prochaska 1998; Ledoux et al. 2006; Murphy et al. 2007). Figure 6*a* presents [M/H] values plotted against the Δv_{90} statistic for the GRB-DLAs and the full QSO-DLA sample. The QSO-DLAs shown in Figure 6*a* exhibit the correlation reported by previous authors (Wolfe & Prochaska 1998; Ledoux et al. 2006). It is not a tight trend, however, and we suspect that several physical factors (e.g., a mass/metallicity relation and variations with sight-line impact parameter and galaxy inclination) contribute to produce the observed distribution. Similar to the Δv_{90} distribution (Fig. 6*a*), we find that the GRB-DLAs track the locus defined by the QSO-DLAs. Adopting the upper limit to [M/H] as a value, we report a Pearson correlation coefficient of 0.4. We conclude that there is only tentative evidence for a correlation between Δv_{90} and [M/H] for the GRB-DLAs.

In Figure 6*b*, we present the W_{1526}, [M/H] pairs for the two populations. The QSO-DLA data exhibit a remarkably tight correlation. These are well described by a power law,

$$[\mathrm{M/H}] = a + b \log (W/1\ \text{Å}), \qquad (1)$$

with best-fit parameters $a = -0.92 \pm 0.05$ and $b = 1.41 \pm 0.10$. For this fit, we have assumed equal weights for all of the data points, and we have restricted the sample to $W_{1526} < 1.4$ Å to ignore the outliers at large W_{1526} values. If we include all of the data points (with equal weighting), we derive $a = -1.00 \pm 0.05$ and $b = 1.27 \pm 0.10$. Although the data scatter about this power law, the trend is considerably tighter than the correlation between Δv_{90} and [M/H]. In fact, it is the tightest correlation known between metallicity and any other property of the QSO-DLAs. The small scatter (≈0.25 dex) is especially impressive, given that

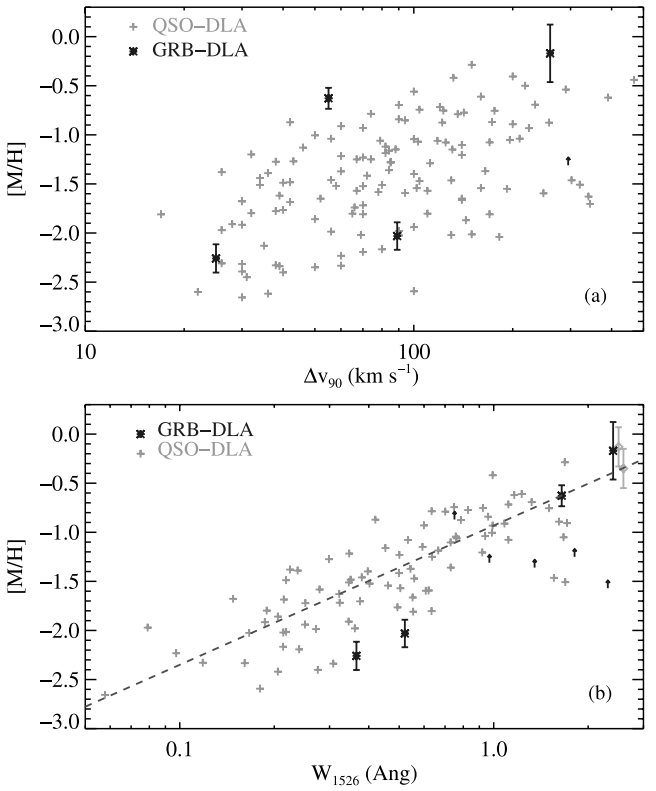

FIG. 6.—Correlations between the gas kinematics and metallicity. (*a*) Pairs of Δv_{90}, [M/H] values for the QSO-DLAs (*plus signs*) and GRB-DLAs (*stars*). The GRB-DLAs with lower limits to [M/H] have saturated metal line profiles. The QSO-DLAs exhibit a previously discussed correlation (Wolfe & Prochaska 1998; Ledoux et al. 2006), and the GRB-DLAs appear to trace the same locus. (*b*) Comparison of [M/H] with W_{1526}. The QSO-DLAs exhibit a remarkably tight trend, described by the dashed line, $[\mathrm{M/H}] = -0.92 + 1.41 \log (W_{1526}/1\ \text{Å})$. The GRB-DLAs also appear to show a correlation that may be offset or steeper than the QSO-DLAs, but this conclusion is complicated by the preponderance of lower limits. Finally, the diamonds show the [M/H], W_{1526} values for the Lyman break galaxies. Although their correspondence with the QSO-DLA trend may be a coincidence, it is suggestive that large W_{1526} values are related to galactic outflows. [*See the electronic edition of the Journal for a color version of this figure.*]

≈0.15 dex is expected from observational uncertainty in the [M/H] measurements ($N_{\mathrm{H\ I}}$ error). It is a rather surprising trend, because the kinematics of the gas that determines [M/H] are better described by the Δv_{90} statistic, yet Figure 6*a* shows this correlation has much greater scatter. Put another way, the line profiles with $W_{1526} > 0.3$ are highly saturated and should not be expected to reflect the gas metallicity (Fig. 3).

This is not to imply that the W_{1526} values are strictly independent of [M/H]. For example, an optical depth profile characterized by shallow, decreasing wings extending to large velocity (e.g., a Lorentzian profile) would yield larger W_{1526} for larger $N(\mathrm{Si}^+)$. On the other hand, a velocity field with a sharp cutoff (e.g., a Gaussian random field) would be insensitive to [M/H]. Furthermore, the peak optical depth value is a function of both [M/H] and $N_{\mathrm{H\ I}}$, and the QSO-DLA data presented in Figure 6*b* span a factor of ≈1.5 dex in $N_{\mathrm{H\ I}}$ value. Therefore, the results on the QSO-DLAs in Figure 6*b* indicate an underlying physical mechanism that causally connects [M/H] and W_{1526}. The GRB-DLAs also show a trend between W_{1526} and [M/H], although its characterization is complicated by the many lower limits to [M/H]. A qualitative assessment of the current results suggests either an offset between the trends for the two populations and/or a steeper power law for the GRB-DLAs. If one interprets the QSO-DLA trend in terms of a mass-metallicity relation (§ 5.3), the offset of

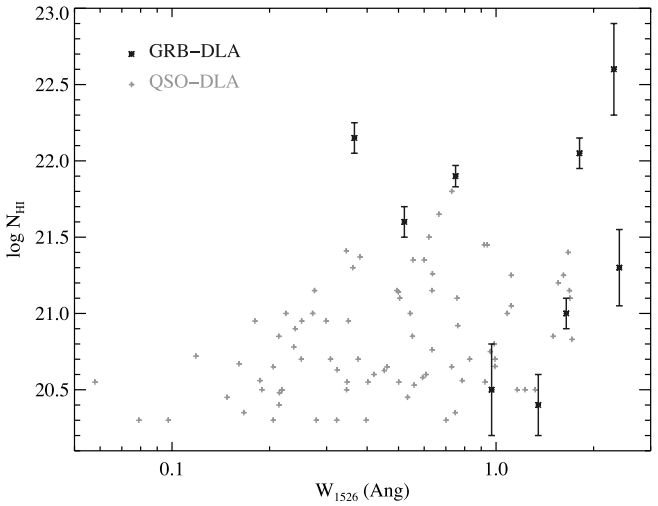

FIG. 7.—Pairs of W_{1526}, $N_{\rm H\,I}$ values for the QSO-DLAs (*gray*) and GRB-DLAs (*black*). Regarding the QSO-DLAs, systems with larger W_{1526} show a larger $N_{\rm H\,I}$ value on average, yet the correlation shows large scatter. Similarly, the GRB-DLA sample is characterized by a large scatter without any obvious trend. Although the $N_{\rm H\,I}$ value and metallicity [M/H] contribute equally to the Si^+ column density and presumably W_{1526}, the latter is tightly correlated only with metallicity. Note that the measurements of W_{1526} and $N_{\rm H\,I}$ values for the QSO-DLAs are typically less than a few times 10 m Å and 0.2 dex, respectively. [*See the electronic edition of the Journal for a color version of this figure.*]

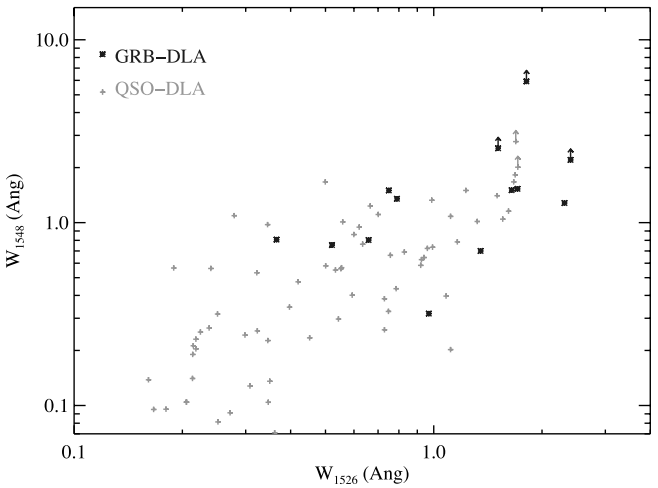

FIG. 8.—Gas kinematics of high ions (W_{1548}) compared against low-ion kinematics (W_{1526}) for the QSO-DLAs (*gray*) and GRB-DLAs (*black*) samples. The two quantities are clearly correlated for the QSO-DLAs, whereas the GRB-DLAs exhibit too small a dynamic range to robustly exhibit any trend. Note that the W_{1526} and W_{1548} values for the QSO-DLAs have uncertainties of less than a few times 10 mÅ. [*See the electronic edition of the Journal for a color version of this figure.*]

GRB-DLAs from the locus of "normal" galaxies at high z may remind the reader of a similar offset seen between GRB host galaxies and normal star-forming galaxies in the metallicity-luminosity plane at low z (Prochaska et al. 2004; Modjaz et al. 2007). In both cases, the offset may reflect the fact that the GRB phenomenon occurs in galaxies at a special (e.g., early time) epoch.

Irrespective of the physical origin of the correlation, the results presented in Figure 6*b* indicate that one may use W_{1526} as a proxy for metallicity, especially if applied to a sample of data points instead of individual systems. We find that a sample of at least 10 QSO-DLA systems gives an average logarithmic metallicity derived from the observed W_{1526} values and equation (1) that lies within 20% of the actual value for 95% of random trials. Emboldened by this result, we apply equation (1) to the GRB-DLAs, but offsetting [M/H] by $\delta_{\rm MH}$ to allow for an offset between the GRB-DLA and the QSO-DLA trends. We derive an average logarithmic metallicity for the GRBs of $\langle[{\rm M/H}]\rangle = -0.8 + \delta_{\rm MH}$.

We have also examined trends between W_{1526} and the H I column density (for Δv_{90} vs. $N_{\rm H\,I}$; see Wolfe & Prochaska 1998; Wolfe et al. 2005). Figure 7 presents the W_{1526}, $N_{\rm H\,I}$ pairs for the QSO-DLAs and GRB-DLAs. The two quantities are correlated in that the median $N_{\rm H\,I}$ value increases with W_{1526}. Furthermore, there are no sight lines with low W_{1526} and large $N_{\rm H\,I}$ values. For sight lines with $W_{1526} > 0.3$ Å, however, we observe a wide range of $N_{\rm H\,I}$ values for any given W_{1526} value. The large observed scatter contrasts with the [M/H], W_{1526} trends in the bottom panel of Figure 6*b*, even though $N(Si^+)$ is the product of [M/H] and $N_{\rm H\,I}$. We conclude that only [M/H] is physically tied to the gas kinematics expressed by the W_{1526} statistic.

4.3. *High-Ion Gas: W_{1548}*

It is difficult to measure the 90% velocity interval for C IV in GRB-DLAs because the C IV doublet is often saturated. Therefore, we have examined the rest equivalent width of the C IV 1548 transition, W_{1548}. These are plotted against W_{1526} in Figure 8. Even though unsaturated low-ion profiles do not closely track the C IV line profiles in QSO-DLAs (i.e., component by component; Wolfe & Prochaska 2000a), there is a strong correlation between their low- and high-ion kinematics. Wolfe & Prochaska (2000b) have interpreted this global correlation as an indication that the gas traces the same gravitational potential (see also Maller et al. 2003).

The GRB-DLAs also exhibit a significant correlation between W_{1526} and W_{1548}. However, one also finds that the W_{1548} values of the GRB-DLAs are systematically larger than those for the QSO-DLAs. Similarly, W_{1548} correlates with the ISM metallicity for both samples. The correlation between W_{1548} and W_{1526} in the GRB-DLAs suggests that their velocity fields are at least coupled. This assertion is further supported by the coincidence of C IV and Si II λ1526 absorption at some velocities (Prochaska et al. 2007b). Therefore, investigations of the velocity field of one ion give insight into the other.

5. DISCUSSION

5.1. *Summary of Results*

The results presented in § 4 can be summarized as follows:

1. The distributions of Δv_{90} values (the velocity interval encompassing 90% of the gas) from QSO-DLAs and GRB-DLAs are similar. Both samples exhibit median $\Delta v_{90} \approx 80$ km s^{-1}, with a significant tail, extending to several hundred km s^{-1} (Fig. 4*a*).
2. In contrast to the Δv_{90} statistic, the GRB-DLAs exhibit systematically larger W_{1526} measurements than the QSO-DLAs (Fig. 4*b*).
3. The QSO-DLAs show a correlation between Δv_{90} and metallicity [M/H] (Fig. 6*a*).
4. There is a remarkably tight correlation between W_{1526} and metallicity [M/H] for the QSO-DLA sample. The correlation is well described by a power law, $[{\rm M/H}] = a + b \log(W_{1526}/1\ \text{Å})$ with $a = -0.92 \pm 0.05$ and $b = 1.41 \pm 0.10$. We observe a possible correlation between metallicity and W_{1526} for the GRB-DLAs. This trend may be offset and/or steeper than the QSO-DLA distribution (Fig. 6*b*).
5. The high-ion and low-ion kinematics traced by W_{1526} and W_{1548} are correlated (Fig. 8).

We now explore the origin and nature of the velocity fields in QSO-DLAs and GRB-DLAs and the implications for the galaxies that produce them.

5.2. *The Nature of Galactic Velocity Fields at High z*

In a star-forming galaxy, there are four principal areas that have unique velocity field characteristics and can contribute to the Δv_{90} and W_{1526} statistics: (1) the neutral ISM, whose motions are dominated by galactic rotation and mild turbulent velocities; (2) H II regions, with velocity fields driven by stellar processes (e.g., winds and supernovae); (3) halo gas clouds, whose kinematics include contributions from gravitational accretion and virialized motions; and (4) galactic-scale outflows driven by supernovae activity in the ISM (e.g., Mac Low & Ferrara 1999) and/or heating by galaxy-galaxy mergers (e.g., Cox et al. 2006). In the following, we examine our observational results within the framework of a model in which the Δv_{90} statistic is dominated by gas in the ambient, neutral ISM[8], while halo dynamics determine the W_{1526} and W_{1548} measurements. In addition, we propose that the W_{1526} and W_{1548} statistics occasionally trace velocity fields representative of galactic-scale outflows.

This two-component scenario (neutral ISM + halo gas) is neither an original nor a provocative interpretation of absorption-line systems arising in galaxies (e.g., Mo & Miralda-Escude 1996; Kauffmann 1996; Haehnelt et al. 1998; McDonald & Miralda-Escudé 1999; Maller et al. 2001, 2003). Indeed, this is also the favored model for gas in the Milky Way (e.g., Spitzer 1990; Savage et al. 1997) and Magellanic Clouds (e.g., Lehner & Howk 2007). Furthermore, the model has been invoked for a wide range of quasar absorption-line observations, including the impact parameter distribution of Mg II systems from their host galaxies (Bergeron & Boisse 1991; Lanzetta & Bowen 1990; Lanzetta & Bowen 1992; Steidel 1993) and C IV absorption by galaxies (Chen et al. 2001; Wolfe & Prochaska 2000b; Maller et al. 2003). We demonstrate that our observations support this model, and we derive new insights into the gas dynamics of high-z galaxies.

Within this ISM/halo scenario, the Δv_{90} statistic traces the kinematics of the ambient ISM, i.e., the optical depth of the gas external to the neutral ISM contributes less than 10% of the total. In the context of QSO-DLAs, this is reasonable because (1) the large $N_{\rm H\,I}$ values that define a DLA may require that the sight lines intersect the ambient ISM, and (2) one expects halo gas to be predominantly ionized (e.g., Mo & Miralda-Escude 1996), whereas the majority of gas in QSO-DLAs is neutral (Vladilo et al. 2001; Prochaska et al. 2002). We now demonstrate that observations of the GRB-DLAs directly connect the neutral ISM with the Δv_{90} statistic.

Figure 9 plots pairs of strong resonance line transitions (one weak, one strong) against a fine-structure transition for four GRB-DLAs observed at high spectral resolution. In all four cases, the fine-structure absorption lines trace only the gas that dominates the integrated optical depth, i.e., the gas revealed by the weak transitions. Prochaska et al. (2006) showed that fine-structure absorption in the GRB-DLAs is due to UV pumping by radiation from the GRB event and its afterglow. For the GRB-DLAs shown here, the presence of fine-structure absorption dictates that this gas is located within $\approx$1 kpc of the burst. Furthermore, the GRB-DLAs also show Mg I absorption coincident with the fine-structure lines (Prochaska et al. 2007b). This requires the gas to lie at $\gtrsim$100 pc to avoid being photoionized by the GRB afterglow (Prochaska et al. 2006, 2007a). The overall implication is that gas comprising 90% of the integrated optical depth lies between $\approx$100 pc and $\approx$1 kpc from the GRB, i.e., within the nearby ISM.[9]

In summation, the GRB-DLA observations give empirical confirmation that the Δv_{90} values reflect the kinematics of the neutral ISM.

Having established a direct association between the Δv_{90} values and the ISM, it is reasonable to assume that these values trace the rotational dynamics and turbulent fields within high-z galaxies. This is especially the case for systems with $\Delta v_{90} < 200$ km s^{-1}; larger Δv_{90} values may be better interpreted as sight lines through multiple galaxies or even supernovae winds (Nulsen et al. 1998). Because the turbulent velocities in neutral gas are generally small ($\sigma_{\rm turb} \approx 10$ km s^{-1}), sight lines with $\Delta v_{90} > 20$ km s^{-1} should be dominated by differential rotational along the sight line or peculiar motions of multiple massive clumps (Haehnelt et al. 1998; Maller et al. 2001). It is natural, therefore, to compare the Δv_{90} distributions of GRB-DLAs and QSO-DLAs in terms of dynamical masses. Before drawing such conclusions using the Δv_{90} distributions, however, one must examine the effects of differences in sight-line configuration (Fig. 2).

The GRB-DLA sight lines are restricted to travel through approximately half of the galaxy and are expected to have a smaller impact parameter than the average QSO-DLA sight line. The latter point is supported by the higher H I column densities, metallicities, and depletion levels observed for GRB-DLA sight lines (Prochaska et al. 2007a). These two effects will compete against each other if differential rotation explains the Δv_{90} statistic. On the one hand, a reduced sight line leads to an underestimate of Δv_{90} because one does not probe all of the gas along the sight line. This effect should be small, however, because even a full sight line will only probe approximately one quadrant of a rotating disk (Prochaska & Wolfe 1997). The correction would be larger for a random velocity field, but still less than a factor of 2. It is only if the velocity fields are dominated by a symmetric infall/outflow that the effect would be large. Such velocity fields, however, are unlikely to describe the neutral ISM of high-z galaxies. The other geometric effect—smaller average impact parameter—will imply larger Δv_{90} values (e.g., Prochaska & Wolfe 1997). This effect is likely to dominate and, if anything, we expect that the GRB-DLAs would be biased to higher Δv_{90} values than the QSO-DLAs for sight lines penetrating the same parent population of galaxies.

We conclude, therefore, that the observed Δv_{90} distributions indicate that the galaxies hosting QSO-DLAs and GRB-DLAs have similar mass distributions. There is at least circumstantial evidence in support of this conclusion. In particular, the median luminosity of GRB-DLAs host galaxies is low, approximately $L_*/5$ at $z \sim 1$ (Le Floc'h et al. 2003). Although very few QSO-DLAs have been successfully imaged at $z > 2$ (Møller et al. 2002), the theoretical expectation is that the majority will also be subluminous (Haehnelt et al. 2000; Maller et al. 2000; Nagamine et al. 2007), and the average luminosity at $z < 1$ is $L \sim L_*/2$ (Chen & Lanzetta 2003). Similarly, neither sample has shown evidence for a large fraction of bright galaxies (Le Floc'h et al. 2003; Colbert & Malkan 2002). Altogether, we conclude that the host galaxies of GRB-DLAs and QSO-DLAs have comparable masses. Adopting recent results on the latter population, we infer dark matter halo masses of $\lesssim 10^{12}\ M_\odot$ for the GRB-DLAs (Boucle et al. 2005; Cooke et al. 2006; Nagamine et al. 2007).

The assertion that GRB-DLA and QSO-DLA host galaxies have similar masses is immediately challenged by our observation that GRB-DLAs show systematically larger W_{1526} values (Fig. 4*b*). To address this issue, we must identify the origin of the velocity fields contributing to W_{1526}. There are two factors that contribute to the W_{1526} statistic: the number of clouds intersected by the sight line and the relative velocities of these clouds. The

[8] Note that we describe the neutral ISM in the framework of a "disk," but that most of our conclusions are independent of the ISM morphology.

[9] The absence of H_2 absorption in this gas (Tumlinson et al. 2007) also indicates that we are probing the ambient ISM and not the local star-forming region (i.e., the molecular cloud).

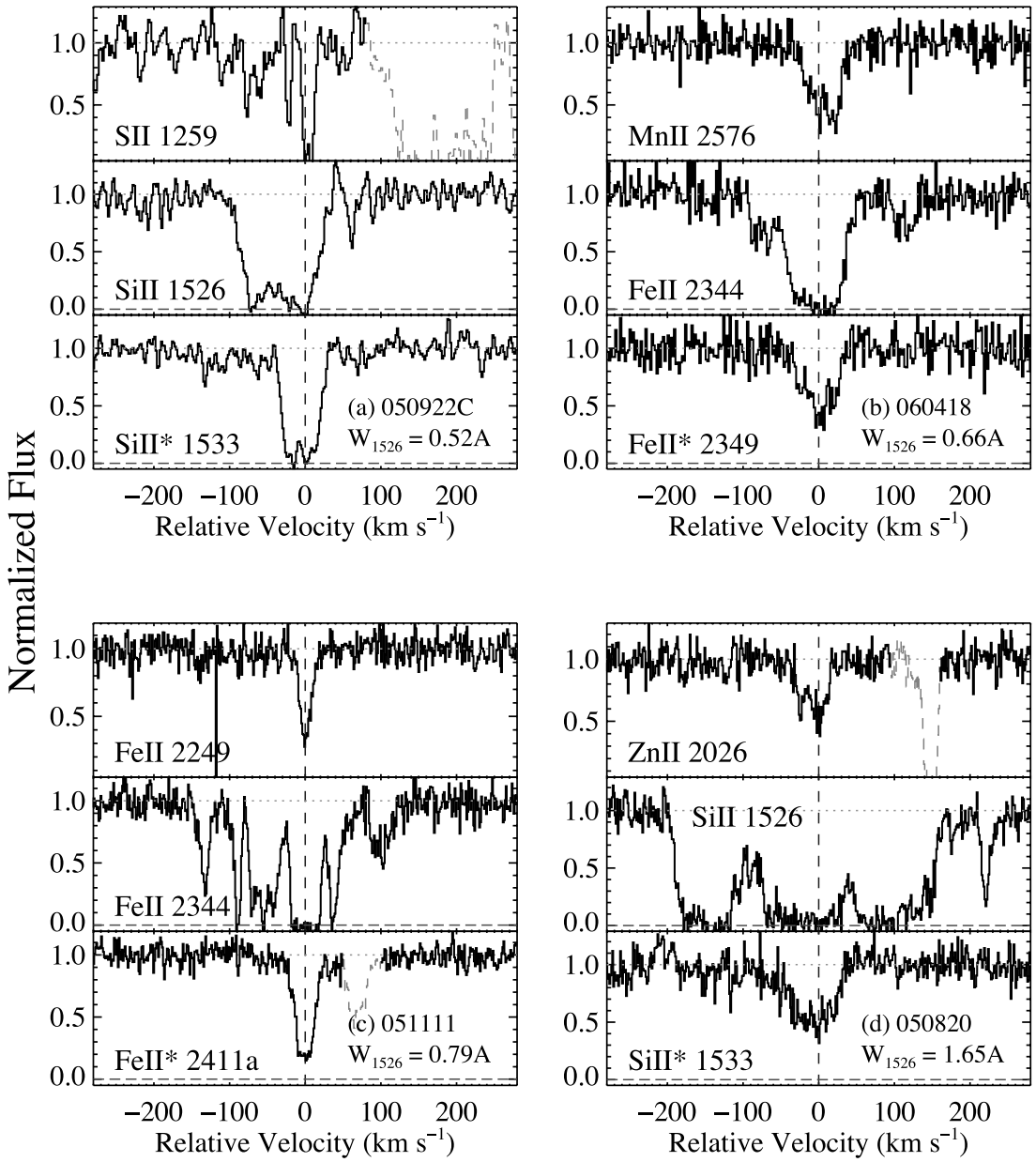

FIG. 9.—One weak line (*top panels*), one strong line (*middle panels*), and one fine-structure transition (*bottom panels*) for four GRB-DLAs observed at high spectral resolution. (*a*) GRB-DLA /050922C, (*b*) GRB-DLA /060418, (*c*) GRB-DLA /051111, and (*d*) GRB-DLA /050820. In all four GRB-DLAs, the fine-structure optical depth profile closely matches that of the weak transition. Because this gas must lie within ≈1 kpc of the GRB afterglow, these observations indicate that the Δv_{90} statistic is determined by the velocity field of the ISM surrounding the GRB. In contrast, there are clouds in the wings of the strong transitions that do not show significant fine-structure absorption and must therefore lie at a distance ≳1 kpc from the GRB afterglow. Because the fine-structure absorption defines the systemic velocity of the ISM, the unique geometry of the GRB-DLA sight lines allows one to investigate gas with velocities indicative of outflow (negative) or infall (positive). This experiment offers an unprecedented view into the nature of gas kinematics in high-z galaxies. [*See the electronic edition of the Journal for a color version of this figure.*]

total velocity field is a convolution of the relative velocity field within each environment, giving rise to Si^+ and the relative velocities between the environments. We emphasize that even highly ionized gas can have trace quantities of Si^+ that would be revealed by the strong Si II λ1526 transition (e.g., Prochaska 1999).

Returning to Figure 9, we can address the contribution of various velocity fields to W_{1526} (note that we have used the strong Fe II 2344 transition as a proxy for Si II 1526 for GRB 051111 and GRB 060418). At small W_{1526} values (Figs. 9*a* and 9*b*), the neutral ISM clearly dominates. In contrast, the two GRB-DLAs with large W_{1526} (Figs. 9*c* and 9*d*) show multiple clouds with relatively low column density and no associated fine-structure absorption. The absence of fine-structure absorption places these clouds at ≳1 kpc from the GRB afterglow (Prochaska et al. 2006; Chen et al. 2007). Note that this is true even though the column densities of these components are small compared to the total because the resonance and fine-structure transitions have similar oscillator strengths. Therefore, this gas cannot be associated with star formation processes local to the GRB (e.g., stellar winds and supernovae). The gas is either within the ISM, but at much larger distance than the gas that dominates the integrated optical depth, or it lies outside the ISM altogether (i.e., halo gas or the ISM of a companion galaxy). We prefer to associate the gas with the galactic halo because (1) the velocities are large (up to hundreds of km s^{-1}) compared to random and dynamical motions for the neutral ISM of galaxies; (2) if the W_{1526} statistic tracked dynamics in the ISM, then a very large metallicity gradient may be required for the Δv_{90} statistic to be insensitive to these motions; (3) there is high-ion

absorption (e.g., Si IV and C IV; Fig. 1) coincident with many of the low column density Si^+ components; and (4) the ionic ratios of some components indicate that they are highly ionized (Dessauges-Zavadsky et al. 2006). An example of the last point is revealed in Figure 1 by the cloud at $v \approx +200$ km s^{-1}. This cloud has $\log [N(O^0)/N(Si^+)] = +0.50 \pm 0.05$, even though O is at least 1 dex more abundant than Si in every astrophysical environment known. The only viable explanation for observing $O^0/Si^+ \ll (O/Si)_\odot$ is that the gas is highly ionized.

Granted that gas beyond the ISM dominates the W_{1526} statistic, the next issue is to examine the nature of its velocity field. This may include virialized motions, gravitational accretion (Mo & Miralda-Escude 1996; McDonald & Miralda-Escudé 1999), and outflows from galactic feedback (Dong et al. 2003; Cox et al. 2006). The latter two processes imply organized flows that would be revealed by the observations if we knew the systemic velocity of the galaxy. For the GRB-DLAs, we can measure the systemic redshift from nebular emission lines (e.g., Thoene et al. 2006), but the absorption-line data also yield a direct measurement, the line centroid of the fine-structure transitions. Because this gas occurs within $\approx$1 kpc for the GRB-DLA, it establishes the velocity of the neutral ISM. Examining the line profiles of Figures 9*c* and 9*d* in this light, we note that the Si^+ gas shows both positive and negative absorption in the case of GRB-DLA 050820, but predominantly negative velocities for GRB-DLA 051111 (where, again, we have used Fe^+ as a proxy for Si^+). Therefore, one example exhibits motions reflective of a random (i.e., virialized) velocity field, and the other inspires an outflow interpretation (see also Thoene et al. 2006). It is too early to draw generic conclusions about the velocity fields of GRB-DLAs, but future observations akin to Figure 9 will offer an unprecedented view into the nature of gas kinematics at high z.

Let us now address the offset in the W_{1526} distributions between the GRB-DLAs and QSO-DLAs (Fig. 4*b*). Could the offset be explained by differences in sight-line configurations? As with the Δv_{90} values, there are competing effects. The bias to smaller impact parameter will only be important if the Si^+ velocity fields have significant variations on kpc scales. This could occur if the majority of gas is located near star-forming regions, i.e., the origin of the GRB sight line. If the Si^+ gas is distributed throughout the halo (i.e., tens of kpc), then an impact parameter bias should be unimportant. Meanwhile, if the velocity field has significant contribution from infall or outflow, then restricting the GRB-DLA sight lines to originate from within the ISM leads to a systematic underestimate. Therefore, sight-line geometry will bias the W_{1526} statistic to larger values for the GRB-DLAs only if the velocity field has significant variations on kpc scales and is asymmetric. Numerical simulations do indicate that gas being accreted tends to fall in along radial orbits (A. Dekel 2006, private communication). This may imply larger W_{1526} values for sight lines originating at the center of the galaxy (GRB-DLAs) as opposed to a large impact parameter (QSO-DLAs). While differences in sight-line configurations may contribute to the differences in W_{1526} between QSO-DLAs and GRB-DLAs, we contend that the observed differences in the W_{1526} distributions for GRB-DLAs and QSO-DLAs reflect actual differences in the gas kinematics of their host galaxies.

A possible explanation for larger W_{1526} values in GRB-DLAs is that their host galaxies are significantly more massive. There are two arguments against this assertion. First, the Δv_{90} distributions of the QSO-DLAs and GRB-DLAs are similar (Fig. 4*a*). While the W_{1526} statistic may be a better tracer of the gravitational potential (see below), the Δv_{90} statistic should also distinguish between large differences in dark matter halo masses. Second, direct imaging of GRB host galaxies reveals that they have low luminosity (Le Floc'h et al. 2003; Fruchter et al. 2006), and presumably low mass. We consider it unlikely that the QSO-DLAs have substantially lower luminosity (and mass) than that observed for the GRB-DLAs.

The most likely interpretation for the higher W_{1526} values in GRB-DLAs is that the kinematics of gas contributing to the W_{1526} statistic has a significant contribution from galactic-scale outflows. We are guided to this conclusion in part because the GRB phenomenon is directly linked to active star formation; i.e., GRB host galaxies have systematically higher current star formation rates than QSO-DLA galaxies. One observes that GRB host galaxies have star formation rates that are large for their luminosity (Christensen et al. 2004). This characteristic is described as a high specific SFR, and it separates GRB host galaxies from the general population of high-z galaxies. Therefore, a scenario in which processes related to star formation stir the velocity fields traced by Si^+ gas may naturally account for the systematic offset in W_{1526} between QSO-DLAs and GRB-DLAs. These processes may include galactic outflows inspired by major mergers (Cox et al. 2006) or galactic fountains driven by supernovae feedback (Mac Low & Ferrara 1999; Dong et al. 2003). The latter effect may be challenged, however, by the short lifetime expected for GRB progenitors. In this respect, the velocity fields of GRB-DLAs may more resemble the outflows of the Lyman break galaxies (e.g., Pettini et al. 2002). We eagerly await new observations like those presented in Figure 9 to further test these scenarios.

5.3. *Interpreting the Kinematics-Metallicity Correlations in DLAs*

In § 4.2 (Fig. 6), we presented the observed correlations between the kinematic statistics (Δv_{90} and W_{1526}) and the ISM metallicity [M/H]. The Δv_{90}-[M/H] correlation has been previously identified for QSO-DLA samples (Wolfe & Prochaska 1998; Ledoux et al. 2006). Although its scatter is substantial, the statistical significance is high, and Ledoux et al. (2006) report a best-fit power law of the form $[M/H] \propto 1.5 \log \Delta v_{90}$. These authors have interpreted the result in terms of a mass-metallicity relation; i.e., the Δv_{90} statistic traces the gravitational potential of the DLA galaxy. Our results for the GRB-DLAs lend further support to this interpretation. In particular, we have shown that the Δv_{90} statistic is dominated by material near the GRB, i.e., the neutral ISM. Although ISM velocity fields are stirred by supernovae, they are generally dominated by gravitational motions (e.g., rotation, turbulence, and accretion).

A key aspect of the Δv_{90}-[M/H] trend is its large scatter; this cannot be attributed to observational uncertainty alone. We interpret the scatter as a natural consequence of the QAL experiment. If the velocity field is dominated by rotation, then a large scatter results simply from a range of impact parameters and disk inclinations (e.g., Prochaska & Wolfe 1997). In this case, only the lower bound of the Δv_{90}, [M/H] locus would describe the average rotation speed of galaxies at a given metallicity. Similarly, if the velocity field results from turbulence or accretion, then Δv_{90} will be sensitive to the number of clouds intersected by the sight line. In this scenario, however, one would require large variations in the number of "clouds" intersected by sight lines, which is not entirely supported by the observations (e.g., Prochaska & Wolfe 1997).

In contrast to the Δv_{90}-[M/H] trend, the W_{1526}, [M/H] pairs for the QSO-DLAs follow a very tight correlation (Fig. 6*b*). In fact, approximately half of the scatter can be attributed to observational uncertainty (especially in the $N_{H\,I}$ values). In several

respects, this is a stunning result. The [M/H] values represent the average metallicity along the entire sight line, which is dominated, of course, by the gas corresponding to the majority of the integrated optical depth, i.e., the gas that defines the Δv_{90} statistic. In contrast, gas that makes a negligible contribution to the measured metallicity can dominate the W_{1526} statistic (Fig. 9). Furthermore, we have shown that [M/H] is set by gas local to the ISM of the galaxy, whereas the W_{1526} statistic has significant contribution from gas external to the ISM. Indeed, quasar absorption lines are frequently associated with halo gas surrounding a galaxy (e.g., Bergeron & Boisse 1991; Steidel 1993; Chen et al. 2001; Charlton & Churchill 1998). Therefore, in the DLAs we reach the rather surprising conclusion that the local ISM properties (metallicity) are tightly correlated with the large-scale velocity field.

Let us now comment on the origin of the W_{1526}-[M/H] trend. The first point to stress is that we derive a power law similar to that observed for the Δv_{90}, [M/H] pairs in QSO-DLAs (see also Murphy et al. 2007). We conclude that the kinematics-metallicity trends have the same physical origin. One may gain insight by comparing our trend with the velocity-metallicity correlations observed for other galactic populations. Dekel & Woo (2003) have found that the velocity dispersion V in dwarf and low-luminosity low surface brightness galaxies at $z = 0$ correlates with the stellar mass M_*: $V \propto M_*^{0.24}$. Furthermore, their compilation shows a tight correlation between metallicity and stellar mass, $\mathrm{M/H} \propto M_*^{0.40}$, implying a metallicity-velocity correlation, $\mathrm{M/H} \propto V^{1.66}$. The correspondence between the kinematics-metallicity trend of local low-mass galaxies with that of the QSO-DLAs is remarkable. Although one refers to this trend locally as a mass-metallicity relation, it is important to stress that simple scaling laws do not predict the observed trend. Dekel & Woo (2003) have shown that in a closed-box model the metallicity is independent of stellar mass; indeed, this follows observations for massive, high surface brightness galaxies (e.g., Tremonti et al. 2004). Therefore, Dekel & Woo (2003) argued that the mass-metallicity trend observed for lower mass galaxies requires supernova feedback (but see also Lee et al. 2006; Tassis et al. 2008). In this respect, therefore, one may speculate whether the velocity fields observed in the QSO-DLAs represent gravitational dynamics or feedback processes. Let us now consider arguments for and against each interpretation.

There are several arguments supporting the interpretation of Figure 6 in terms of a mass-metallicity correlation, i.e., that the velocity fields trace the gravitational potential. First, the observed slopes of the Δv_{90} and W_{1526}-[M/H] trends follow the same trends as local dwarf and low-luminosity, low surface brightness galaxies (Dekel & Woo 2003), whose velocity dispersions presumably reflect their gravitational potentials. Second, the large scatter in the Δv_{90}-[M/H] trend can be explained by variations in impact parameter and inclination through the DLA galaxies. Third, a tight trend is reasonable for W_{1526}, [M/H] pairs if the W_{1526} statistic is dominated by halo dynamics. For virialized motions characterized by a velocity dispersion σ_{virial}, $W_{1526} \propto n_{\mathrm{cld}}^{1/2}\sigma_{\mathrm{virial}}$, and the scatter in this quantity will be small for a given velocity dispersion σ_{virial} if the number of clouds penetrated by the sight line $n_{\mathrm{cld}} \gg 1$. The latter point is supported by the observations (e.g., Fig. 1). Fourth, the Si II 1526 profiles of at least some GRB-DLAs show both negative and positive velocities relative to the systemic (Fig. 9). This is expected for gas that traces a virialized (random) velocity field. Finally, Möller et al. (2004) have noted that the only DLAs that have been successfully imaged at $z \gtrsim 2$ also have high metallicity, suggesting that stellar mass correlates with enrichment.

There are two counterarguments to interpreting the Δv_{90} and W_{1526} statistics as tracers of the gravitational potential of individual dark matter halos. First, it may be unrealistic to explain velocity widths that exceed several hundred km s^{-1} in terms of a single galactic potential. At very large Δv_{90} or W_{1526} values, therefore, we expect that additional velocity fields contribute. These could include galactic-scale outflows, but also the peculiar motions of multiple galaxies along the sight line (e.g., Maller et al. 2001). Second, Boucle et al. (2006) have reported an anticorrelation between Mg II equivalent width[10] and the cluster length of these absorbers (a subset includes DLAs; G. Prochter et al. 2006, in preparation) with large red galaxies (LRGs). These authors have interpreted this result in terms of a wind scenario: systems exhibiting larger equivalent widths occur in less massive, starbursting galaxies. We note, however, several caveats to applying their interpretation to the DLAs: (1) the Mg II absorbers have $z < 1$ and may have very different characteristics (star formation rates, metallicity, and gas content) than the $z > 2$ QSO-DLAs that are plotted in Figure 6, and (2) Zibetti et al. (2007) find the integrated light of galaxies corresponding to Mg II absorbers is independent of equivalent width.

Now consider the evidence in favor of interpreting the W_{1526} statistic (and perhaps Δv_{90}) as galactic-scale outflows. First, as noted above, the trend of decreasing correlation length with increasing equivalent width offers at least qualitative evidence for a wind scenario (Boucle et al. 2006). Second, the line profiles of some strong Mg II absorbers are consistent with that expected for symmetric outflows (Bond et al. 2001). Third, if star formation drives galactic-scale outflows, then one may expect a correlation between metallicity and W_{1526}. It may be difficult to precisely derive the observed trend ($[\mathrm{M/H}] \propto 1.5 \log W_{1526}$) from first principles, but we cannot rule out such a scenario. Fourth, we find that Lyman break galaxies (Pettini et al. 2002; Steidel et al. 2004) lie directly on the W_{1526}-[M/H] trend of the QSO-DLAs (Fig. 6*b*, *diamonds*).

Given that the LBG gas kinematics are dominated by outflows (Pettini et al. 2002), the correspondence between the LBG data and the QSO-DLA trend is at least suggestive that outflows may play a role in shaping the observed correlation. The comparison with the QSO-DLAs may not be appropriate, however, because the LBG sight line is restricted to originate at the central, star-forming region of the galaxy. This implies a special impact parameter and one that presumably probes only half of the total velocity field. In these respects, a comparison with the GRB-DLAs is more appropriate, and the correspondence with the QSO-DLA trend may be simple coincidence. We do note, however, that Heckman et al. (2000) observe an empirical correlation between the equivalent width of the Na I transition and the galaxy mass in low-redshift starburst galaxies.

There are several arguments against interpreting the W_{1526} measurements as galactic-scale outflows. First, the similarity in the W_{1526} and Δv_{90}-[M/H] trends would require one to interpret both statistics in terms of outflows (or invoke coincidence). In turn, one would have to argue that these winds have gas with large neutral fractions (Prochaska et al. 2002) and significant cross section–to–gas ratios, with $N_{\mathrm{H\,I}} > 10^{21}$ cm^{-2} (e.g., Schaye 2001). Second, we believe a galactic-scale outflow scenario would be severely challenged to reproduce the tight correlation observed for W_{1526} and metallicity. Assuming outflows are generally

[10] In absorbers where one observes both the Si II 1526 transition and the Mg II doublet, one finds that the line profiles track each other very closely. As such, their equivalent widths are highly correlated and roughly scale as the inverse of their wavelengths: $W_{1526} \approx W_{2796}\lambda_{1526}/\lambda_{2796}$ (in detail, we find $W_{2796} \approx 3W_{1526}$).

collimated, the W_{1526} statistic should exhibit a wide range of values for a given wind speed as a function of the sight-line configuration (i.e., impact parameter and inclination).

Furthermore, the W_{1526} value is given by the internal dynamics of the wind (i.e., its turbulence), because it is a relative measure independent of the systemic velocity. It is not obvious that this quantity could be tightly correlated with metallicity. Third, there are at least some GRB-DLAs for which the W_{1526} velocity field is not strictly consistent with outflows (Fig. 9). Fourth, mass-metallicity relations have been identified for numerous galaxy populations at a range of redshifts (Dekel & Woo 2003; Tremonti et al. 2004; Kobulnicky & Kewley 2004; Savaglio et al. 2005; Erb et al. 2006). It would be very remarkable for the QSO-DLAs to exhibit a tight velocity-metallicity trend that was unrelated to a mass-metallicity correlation. Fifth, we question a scenario that requires galactic-scale outflows in all galaxies tuned to give both low and large W_{1526} values with such small scatter. Sixth, comparisons of Mg II absorption-line profiles with H II emission-line kinematics are inconsistent with a wind scenario and support dynamical motions (Steidel et al. 2002). Finally, while observers are quick to invoke outflows to explain extreme velocity fields, we question whether outflows can reasonably explain widths approaching and in excess of 1000 km s^{-1}.

On balance, we currently favor the interpretation of the velocity fields in QSO-DLAs as being dominated by gravitational motions, at least for $W_{1526} < 1.5$ Å and $\Delta v_{90} < 200$ km s^{-1}. At large W_{1526} and large Δv_{90}, it is reasonable to expect that additional velocity fields contribute. Indeed, an inspection of Figure 6*b* reveals that the QSO-DLA galaxies with the largest departure from the [M/H]-W_{1526} relation occur at large W_{1526} values. These few QSO-DLAs have especially large W_{1526} for their observed metallicity and/or low metallicity for the observed W_{1526} value. We suspect that the former inference is the correct interpretation and that these systems make contributions to the W_{1526} statistic beyond the halo gas dynamics. These QSO-DLAs are the most viable candidates for sight lines penetrating galactic-scale outflows. This interpretation could also explain the frequency of GRB-DLAs that lie off the QSO-DLA trend. As noted in the previous section, GRB-DLAs have especially large specific star formation rates. Therefore, GRBs may flag galaxies at a time when they are most likely to drive galactic-scale outflows. Given the identification of GRBs with massive, short-lived stars, there may not be sufficient time to drive these winds with supernovae feedback. Instead, one may need to consider merger-driven, galactic outflows.

We wish to thank A. Dekel, A. Maller, D. Lin, E. Ramirez-Ruiz, M. Murphy, P. Bodenheimer, J. Hennawi, S. Ellison, S. Burles, and R. Bernstein for valuable discussions. We thank M. Pettini for kindly providing W_{1526} values for the LBG samples. J. X. P. is partially supported by NASA/*Swift* grant NNG05GF55G and an NSF CAREER grant (AST 05-48180).

REFERENCES

Barth, A. J., et al. 2003, ApJ, 584, L47
Berger, E., et al. 2006, ApJ, 642, 979
Bergeron, J., & Boisse, P. 1991, Adv. Space Res., 11, 241
Bond, N. A., et al. 2001, ApJ, 562, 641
Boucle, N., Gardner, J. P., Katz, N., Weinberg, D. H., Davé, R., & Lowenthal, J. D. 2005, ApJ, 628, 89
Boucle, N., Murphy, M. T., Péroux, C., Csabai, I., & Wild, V. 2006, MNRAS, 371, 495
———. 2007, NewA Rev., 51, 131
Castro, S., et al. 2003, ApJ, 586, 128
Charlton, J. C., & Churchill, C. W. 1998, ApJ, 499, 181
Chen, H.-W., & Lanzetta, K. M. 2003, ApJ, 597, 706
Chen, H.-W., Lanzetta, K. M., & Webb, J. K. 2001, ApJ, 556, 158
Chen, H.-W., Prochaska, J. X., Bloom, J. S., & Thompson, I. B. 2005, ApJ, 634, L25
Chen, H.-W., Prochaska, J. X., Ramirez-Ruiz, E., Bloom, J. S., Dessauges-Zavadsky, M., & Foley, R. J. 2007, ApJ, 663, 420
Christensen, L., Hjorth, J., & Gorosabel, J. 2004, A&A, 425, 913
Colbert, J. W., & Malkan, M. A. 2002, ApJ, 566, 51
Cooke, J., et al. 2006, ApJ, 636, L9
Cox, T. J., et al. 2006, MNRAS, 373, 1013
Dekel, A., & Woo, J. 2003, MNRAS, 344, 1131
Dekker, H., D'Odorico, S., Kaufer, A., Delabre, B., & Kotzlowski, H. 2000, Proc. SPIE, 4008, 534
Dessauges-Zavadsky, M., et al. 2006, A&A, 445, 93
Dong, S., Lin, D. N. C., & Murray, S. D. 2003, ApJ, 596, 930
Erb, D. K., et al. 2006, ApJ, 644, 813
Fiore, F., et al. 2005, ApJ, 624, 853
Fruchter, A. S., et al. 2006, Nature, 441, 463
Fynbo, J. P. U., et al. 2006, A&A, 451, L47
Haehnelt, M. G., Steinmetz, M., & Rauch, M. 1998, ApJ, 495, 647
———. 2000, ApJ, 534, 594
Heckman, T., et al. 2000, ApJS, 129, 493
Herbert-Fort, S., et al. 2006, PASP, 118, 1077
Jedamzik, K., & Prochaska, J. X. 1998, MNRAS, 296, 430
Kauffmann, G. 1996, MNRAS, 281, 475
Kawai, N., et al. 2006, Nature, 440, 184
Kobulnicky, H. A., & Kewley, L. J. 2004, ApJ, 617, 240
Lanzetta, K. M., & Bowen, D. 1990, ApJ, 357, 321
———. 1992, ApJ, 391, 48
Le Floc'h, E., et al. 2003, A&A, 400, 499
Ledoux, C., Petitjean, P., Fynbo, J. P. U., Møller, P., & Srianand, R. 2006, A&A, 457, 71
Ledoux, C., Petitjean, P., & Srianand, R. 2003, MNRAS, 346, 209
Lee, H., et al. 2006, ApJ, 647, 970
Lehner, N., & Howk, J. C. 2007, MNRAS, 377, 687
Mac Low, M.-M., & Ferrara, A. 1999, ApJ, 513, 142
Maller, A., Prochaska, J., Somerville, R., & Primack, J. 2000, in ASP Conf. Ser. 200, Clustering at High Redshift, ed. A. Mazure, O. Le Fèvre, & V. Le Brun (San Francisco: ASP), 430
———. 2001, MNRAS, 326, 1475
———. 2003, MNRAS, 343, 268
McDonald, P., & Miralda-Escudé, J. 1999, ApJ, 519, 486
Metzger, M. R., Djorgovski, S. G., Kulkarni, S. R., Steidel, C. C., Adelberger, K. L., Frail, D. A., Costa, E., & Frontera, F. 1997, Nature, 387, 878
Mirabal, N., et al. 2002, ApJ, 578, 818
Mo, H. J., Mao, S., & White, S. D. M. 1998, MNRAS, 295, 319
Mo, H. J., & Miralda-Escude, J. 1996, ApJ, 469, 589
Modjaz, M., Kewley, L., Kirshner, R. P., Stanek, K. Z., Challis, P., Garnavich, P. M., Greene, J. E., & Prieto, J. L. 2007, AJ, submitted (astro-ph/0701246)
Möller, P., Fynbo, J. P. U., & Fall, S. M. 2004, A&A, 422, L33
Møller, P., Warren, S. J., Fall, S. M., Fynbo, J. U., & Jakobsen, P. 2002, ApJ, 574, 51
Murphy, M. T., Curran, S. J., Webb, J. K., Menager, H., & Zych, B. J. 2007, MNRAS, 376, 673
Nagamine, K., Wolfe, A. M., Hernquist, L., & Springel, V. 2007, ApJ, 660, 945
Nulsen, P. E. J., Barcons, X., & Fabian, A. C. 1998, MNRAS, 301, 168
Pettini, M., Rix, S. A., Steidel, C. C., Adelberger, K. L., Hunt, M. P., & Shapley, A. E. 2002, ApJ, 569, 742
Pettini, M., Shapley, A. E., Steidel, C. C., Cuby, J.-G., Dickinson, M., Moorwood, A. F. M., Adelberger, K. L., & Giavalisco, M. 2001, ApJ, 554, 981
Pettini, M., Smith, L. J., Hunstead, R. W., & King, D. L. 1994, ApJ, 426, 79
Prochaska, J. X. 1999, ApJ, 511, L71
Prochaska, J. X., Chen, H.-W., & Bloom, J. S. 2006, ApJ, 648, 95
Prochaska, J. X., Chen, H.-W., Dessauges-Zavadsky, M., & Bloom, J. S. 2007a, ApJ, 666, 267
Prochaska, J. X., Gawiser, E., Wolfe, A. M., Castro, S., & Djorgovski, S. G. 2003, ApJ, 595, L9
Prochaska, J. X., Henry, R. B. C., O'Meara, J. M., Tytler, D., Wolfe, A. M., Kirkman, D., Lubin, D., & Suzuki, N. 2002, PASP, 114, 933
Prochaska, J. X., Herbert-Fort, S., & Wolfe, A. M. 2005, ApJ, 635, 123
Prochaska, J. X., & Wolfe, A. M. 1997, ApJ, 487, 73
———. 1998, ApJ, 507, 113
———. 2001, ApJ, 560, L33
Prochaska, J. X., et al. 2004, ApJ, 611, 200
———. 2007b, ApJS, 168, 231
Prochter, G. E., Prochaska, J. X., & Burles, S. M. 2006, ApJ, 639, 766

Rao, S. M., Turnshek, D. A., & Nestor, D. B. 2006, ApJ, 636, 610
Razoumov, A. O., et al. 2006, ApJ, 645, 55
Savage, B. D., Sembach, K. R., & Lu, L. 1997, AJ, 113, 2158
Savaglio, S., Fall, S. M., & Fiore, F. 2003, ApJ, 585, 638
Savaglio, S., et al. 2005, ApJ, 635, 260
Schaye, J. 2001, ApJ, 559, L1
Sheinis, A. I., et al. 2000, Proc. SPIE, 4008, 522
Shin, M.-S., et al. 2006, ApJ, submitted (astro-ph/0608327)
Spitzer, L. J., Jr. 1990, ARA&A, 28, 71
Steidel, C. C. 1993, in The Environment and Evolution of Galaxies, ed. J. M. Shull & H. A. Thronson (Dordrecht: Kluwer), 263
Steidel, C. C., Kollmeier, J. A., Shapley, A. E., Churchill, C. W., Dickinson, M., & Pettini, M. 2002, ApJ, 570, 526
Steidel, C. C., & Sargent, W. L. W. 1992, ApJS, 80, 1
Steidel, C. C., Shapley, A. E., Pettini, M., Adelberger, K. L., Erb, D. K., Reddy, N. A., & Hunt, M. P. 2004, ApJ, 604, 534
Tassis, K., Kravtsov, A. V., & Gnedin, N. Y. 2008, ApJ, in press (astro-ph/0609763
Thoene, C. C., Greiner, J., Savaglio, S., & Jehin, E. 2006, ApJ, submitted (astro-ph/0611772)
Tremonti, C. A., et al. 2004, ApJ, 613, 898
Tumlinson, J., Prochaska, J. X., Chen, H.-W., Dessauges-Zavadsky, M., & Bloom, J. S. 2007, ApJ, 668, 667
Vladilo, G., et al. 2001, ApJ, 557, 1007
Vogt, S. S., et al. 1994, Proc. SPIE, 2198, 362,
Vreeswijk, P. M., et al. 2004, A&A, 419, 927
———. 2006, A&A, 447, 145
Watson, D., et al. 2006, ApJ, 652, 1011
Wolfe, A. M., Gawiser, E., & Prochaska, J. X. 2005, ARA&A, 43, 861
Wolfe, A. M., Lanzetta, K. M., Foltz, C. B., & Chaffee, F. H. 1995, ApJ, 454, 698
Wolfe, A. M., & Prochaska, J. X. 1998, ApJ, 494, L15
———. 2000a, ApJ, 545, 591
———. 2000b, ApJ, 545, 603
Wolfe, A. M., Prochaska, J. X., & Gawiser, E. 2003, ApJ, 593, 215
Wolfe, A. M., Turnshek, D. A., Smith, H. E., & Cohen, R. D. 1986, ApJS, 61, 249
Zibetti, S., Ménard, B., Nestor, D. B., Quider, A. M., Rao, S. M., & Turnshek, D. A. 2007, ApJ, 658, 161
Zwaan, M. A., & Prochaska, J. X. 2006, ApJ, 643, 675